Applied Biochemistry and Biotechnology (2023) 195:7465–7482
https://doi.org/10.1007/s12010-023-04452-7

ORIGINAL ARTICLE

Antioxidant and Antidiabetic Activities, and UHPLC-ESI-QTOF-MS-Based Metabolite Profiling of an Endophytic Fungus *Nigrospora sphaerica* BRN 01 Isolated from *Bauhinia purpurea* L

Sai Anand Kannakazhi Kantari[1] · Ranendra Pratap Biswal[2] · Piyush Kumar[1] · Malleswara Dharanikota[1] · Ashok Agraharam[1]

Accepted: 15 March 2023 / Published online: 1 April 2023

Abstract

Diabetes-associated postprandial hyperglycemia is a major risk factor in cardiovascular disease. Since enzyme α-glucosidase is primarily responsible for glucose release during digestion, inhibiting it mitigates post-meal spike in blood glucose level. Metabolites from endophytic fungi could be potential natural inhibitors of this enzyme. Endophytic fungi isolated from *Bauhinia purpurea* L. were screened for their potential antioxidant and antidiabetic activities. Ethyl acetate extract of *Nigrospora sphaerica* BRN 01 (NEE) displayed high antioxidant activity with an IC50 value of 9.72 ± 0.91 µg/ml for DPPH assay and ferric reducing antioxidant power (FRAP) of 1595 ± 0.23 µmol AAE g^{-1} DW. NEE also showed high degree of inhibition of α-glucosidase activity with an IC50 value of 0.020 ± 0.001 mg/ml, significantly greater than the standard drug acarbose (0.494 ± 0.009 mg/ml). Metabolite profiling of NEE was carried using ultra-high-performance liquid chromatography coupled with electrospray ionization quadrupole time-of-flight mass spectrometry (UHPLC-ESI-QTOF-MS) and 21 metabolites identified based on the MS/MS fragmentation patterns. Docking analysis of all 21 identified metabolites was carried out. Of these, 6 showed binding energies higher than acarbose (−6.6 kcal/mol). Based on the analysis of interactions of feruloyl glucose with active site residues of the enzyme, it could be a potential α-glucosidase inhibitor. Metabolites of *Nigrospora sphaerica* BRN 01, therefore, could be potential lead molecules for design and development of antidiabetic drugs.

Keywords *Nigrospora sphaerica* BRN 01 · *Bauhinia purpurea* L. · α-Glucosidase inhibitors · Antioxidant activity · UHPLC-ESI-QTOF-MS · Molecular docking

✉ Ashok Agraharam
aashok@sssihl.edu.in

[1] Department of Biosciences, Sri Sathya Sai Institute of Higher Learning, Brindavan Campus, Bengaluru 560067, Karnataka, India

[2] Department of Chemistry, Sri Sathya Sai Institute of Higher Learning, Prasanthi Nilayam Campus, Puttaparthi 515134, Andhra Pradesh, India

Introduction

Prevalence of type 2 diabetes mellitus (T2DM) has increased sharply during the last three decades, with an estimated 537 million people worldwide diagnosed with diabetes. The prevalence of diabetes among the global population is steadily rising, with the number expected to reach 643 million by 2030. Diabetes has been directly responsible for 6.7 million fatalities in 2021 alone [1]. For early treatment of diabetes and minimizing subsequent consequences like chronic vascular disease, management of postprandial plasma glucose levels is crucial. High level of sugar in the blood termed as hyperglycemia also leads to other complications like kidney failure and neuropathy [2]. Thus, one of the important therapeutic strategies for treating T2DM involves delaying glucose absorption by inhibiting digestive enzymes like α-amylase and α-glucosidase [3]. α-Amylase breaks down starch into smaller chains of glucose called dextrins and maltose. These are then further broken down to glucose by α-glucosidase.

Alpha-glucosidase inhibitors (AGIs) are used as monotherapy drugs or in combination with other antidiabetic drugs like metformin in the treatment of T2DM. AGIs could be administered to patients with impaired glucose tolerance, and are often the drugs of choice for diabetes patients prone to lactic acidosis or hypoglycemia [4]. Furthermore, AGIs are also reported to be a potential calorie restriction mimetics and can play a role in preventing age-related diseases [5]. Use of medications currently available in market such as acarbose, voglibose, and miglitol which target α-glucosidase have been shown to produce gastrointestinal side effects such as nausea, constipation, and diarrhea. Bioactive substances isolated from natural sources have emerged as promising alternatives for management of hyperglycemia with minimal or no side effects [6]. For example, metformin was originally obtained from *Galega officinalis*, a medicinal herb. In a recent study, it was observed that among the 53 plant species analyzed for their α-glucosidase inhibition potential, most of them belonged to family Fabaceae [7]. Most studies carried out till now have focused on screening AGIs from different plant sources. However, endophytic fungi have not been extensively explored as natural sources for AGIs. They are known to produce various novel molecules. The secondary metabolites produced by an endophytic fungus are determined by the environment existing in the host it colonizes. Interestingly, they also have ability to synthesize certain metabolites similar to those produced by the host plant [8].

Bauhinia purpurea, belonging to Fabaceae, has great medicinal potential. In traditional medicine, the leaf, bark, and root of this plant are used to treat asthma, ulcers, stomach disorders, seizures, and rheumatism. In the Amazon region, it is used to treat diabetes. The plant is rich in flavonoids as well as fatty acids, steroids, tocopherols, saponins, and xanthones. It is also rich in bioactive metabolites which exhibit antioxidant, antiulcer, antimicrobial, anticancer, and hypoglycemic activities [9]. Secondary metabolites of endophytic fungi isolated from *Bauhinia purpurea* have however received little attention, and further research could yield important results towards development of potential drugs.

The fungus *Nigrospora* belonging to class ascomycetes is an excellent source of diverse secondary metabolites. Polyketides belong to a major class of metabolites produced by *Nigrospora*. The subtypes mainly include furanones, pyrans, quinones, and monophenyl derivatives. *Nigrospora* produces molecules with rich bioactivity such as griseophenone C, 10-deoxybostrycin, and chermesinone B. These molecules are derived especially from endophytic forms of *Nigrospora* and furthermore studies on their potential bioactivity are needed [10]. The present study investigates the potential of *Nigrospora sphaerica* as a source of AGIs with antioxidant potential.

Materials and Methods

Chemicals and Reagents

2,2-Diphenyl-1-(2,4,6-trinitrophenyl)hydrazyl (DPPH), 2,4,6-tri(2-pyridyl)-s-triazine (TPTZ), p-nitrophenyl-α-D-glucopyranoside, and α-glucosidase from *Saccharomyces cerevisiae* were purchased from Merck. Acetonitrile and water of Optima liquid chromatography–mass spectrometry (LC–MS) grade were obtained from Fisher Chemical. LC–MS additive acetic acid was purchased from Merck. High-performance liquid chromatography (HPLC) grade methanol and ethyl acetate for extraction were procured from Himedia. Potato dextrose agar (PDA) and potato dextrose broth (PDB) were purchased from Himedia.

Collection of Plant Material

Healthy leaves of *Bauhinia purpurea* L. were collected from Bengaluru, India. They were brought to the laboratory immediately after collection and washed thoroughly in distilled water upon arrival. Formal identification of the collected plants was done by the Botanical Survey of India (Deccan Regional Centre, Hyderabad).

Isolation of Endophytic Fungi

Endophytic fungi were isolated from the leaves of *Bauhinia purpurea* L. Using a sterile knife blade, the leaves were cut into 0.5 cm^2 pieces and surface sterilized in 70% ethanol for 5 s, then 90 s in 4% sodium hypochlorite, followed by 10 s of sterile distilled water rinse [11]. The leaf pieces were then transferred to PDA plates under aseptic conditions and incubated at 28 °C for 2–5 days until colonies developed well. Individual colonies were sub-cultured to get pure colonies and were stored at − 20 °C.

Extraction of Extracellular Metabolites

Plugs of pure cultures were inoculated into 100 ml of potato dextrose broth (PDB) in a conical flask and incubated for 21 days. The contents were then homogenized with 10% of methanol and extracted twice with ethyl acetate. Ethyl acetate fraction was subjected to evaporation using a rotary evaporator [12]. The dried extract was preserved at − 20 °C.

Molecular Characterization (rDNA-ITS Sequencing and Phylogenetic Analysis)

Genomic DNA was extracted from the mycelium of isolated endophytic fungi using phenol–chloroform extraction procedure. The amplification of the internal transcribed spacer ribosomal DNA (ITS-rDNA) fragment was carried using PCR with forward primer ITS1 and reverse primer ITS4. These sequences were added to the NCBI GenBank and compared with other sequences there using BLAST searches. The phylogenetic analyses were carried using the MEGA X program [13]. Using the maximum composite likelihood technique, the evolutionary distances were calculated. Neighbor-joining method was then employed to infer the evolutionary history [14], with bootstrap value calculated from 1000 replicates.

Antioxidant Activity

DPPH Assay

The assay was carried out in a 96-well microplate using microplate reader (SpectraMax® M2^e). One hundred fifty microliters of ethyl acetate extracts of endophytic fungi was added to each well with concentrations between 2 and 2000 µg/ml followed by 50 µl of DPPH and incubated for 30 min under dark conditions. Absorbance was taken at 515 nm and the percentage of radicals scavenged is calculated using the equation:

$$\text{DPPH scavenging activity (\%)} : \left[1 - \left(A_s - A_{sc}\right)/A_c\right] \times 100$$

where A_s represents the absorbance of the sample and A_{sc} and A_c represent the absorbance of the sample control and absorbance of control respectively [15].

Ferric Reducing Antioxidant Power Assay

Twenty microliters of 1 mg/ml NEE dissolved in methanol and 280 µl of freshly prepared FRAP reagent were added to each well. Absorbance was measured at 593 nm after 30 min of incubation. Standard curve was plotted using different ascorbic acid concentrations (0.02–0.1 mg/ml). Ferric reducing antioxidant power of NEE was quantified and expressed as µmol ascorbic acid equivalence per gram (µmol AAE/g) of NEE [16].

Antidiabetic Activity

The protocol for α-glucosidase inhibition assay of Bhatia et al. [17] was standardized and used. Into each well of a 96-well plate, 50 µl of 0.1 M phosphate buffer (pH 6.9), 20 µl of ethyl acetate extracts of endophytic fungi at various concentrations (0.01 to 0.05 mg/ml), and 10 µl of 0.2 U/ml α-glucosidase solution were added and incubated for 20 min at 37 °C. Thereafter, substrate (p-nitrophenyl-α-D-glucopyranoside) at 1 mM was added, incubated for 20 min at 37 °C, and reaction terminated by adding 100 µl of 0.1 M Na_2CO_3. Absorbance was recorded at 405 nm using a microplate reader (SpectraMax® M2^e). The following equation was used to compute the percentage of inhibition.

$$\text{Inhibition\%} = 1 - \left[A_s/A_c\right] \times 100$$

where A_s and A_c are defined as the absorbance of the sample and the control, respectively.

IC50 value for the NEE was calculated.

Cytotoxicity Assay

In vitro cytotoxicity of NEE on mammalian cells (RAW 264.7 macrophage cell lines) was carried out using MTT assay [18] with slight modification. Cell viability percentage was calculated using the equation:

$$\text{Viability\%} = \frac{\text{Ac}}{\text{As}} \times 100$$

where A_s and A_c are defined as the absorbance of the sample and the control, respectively.

IC50 value for the NEE was calculated.

Metabolite Profiling by UHPLC–QTOF-MS

Metabolite profiling of NEE was carried out using Agilent UHPLC 1290 infinity coupled to Agilent 6550 Q-TOF LC/MS with a dual jet stream ionization source. Acquisition of data was carried out using Agilent Mass Hunter version B.05.00 software.

NEE was dissolved in methanol to get a final concentration of 0.1 mg/ml. Filtration of NEE was done with Agilent Econofilter polytetrafluoroethylene (PTFE) column with 13 mm diameter and 0.2 µm pore size. Separation of metabolites was carried out using Agilent ZORBAX RRHD Eclipse Plus C18 (3.0 × 100 mm, 1.8 µm) column with elution gradient of 0–2 min, 5% B; 2–7 min, 5–20% B; 7–26 min, 20–50% B; 26–40 min, 50–95% B; 40–45 min, 95% B; and 45–49 min, 5% B using mobile phase A (0.1% HCOOH in water) and mobile phase B (0.1% HCOOH in acetonitrile). Injection volume and flow rate were set at 10 µl and 0.300 ml/min respectively. Quadrupole time of flight parameters was set as nozzle voltage, 1000 V; capillary voltage, 3.5 kV; nebulizer pressure, 35 psi; and drying gas nitrogen, 11 l/min at 250 °C and 350 °C respectively. With the help of the reference standard mix G1969-85,000 (Supelco, Inc.), mass calibration was carried out both in positive and negative ionization modes and the residual error value estimated was found to be only 0.2 ppm. Processing of data was carried out using Agilent Mass Hunter Qualitative Analysis software, version B.070. The compounds were identified based on precise mass and isotope patterns. Confidence in compound identification was represented by the "overall identification score" calculated as a weighted average of the compound's isotopic pattern signals [18].

Library Searching

A database of 850 metabolites was prepared using Agilent Personal Compound Database and Library (PCDL) which included all the metabolites of *Nigrospora* sp., known α-glucosidase inhibitors of fungal origin and important polyphenols. Their structures were either downloaded from the National Centre for Biotechnology Information (NCBI) PubChem database or drawn using ChemBioDraw Ultra 14.0 software. Targeted data mining was carried out using Agilent MassHunter Qualitative Analysis B.7.00 software.

The search process of PCDL produces a match score considering the isotopic abundance and isotopic spacing along with accurate mass of the detected compounds.

Molecular Docking

The human α-glucosidase, maltase-glucoamylase (MGAM), is involved in cleaving α-1–4-glycosidic linkages of linear dextrin molecules resulting in the release of glucose. MGAM belongs to the glycosyl hydrolase family 31 (GH31). MGAM consists of an N-terminal subunit and a C terminal subunit with both having α-glucosidase activity. To understand the human α-glucosidase inhibition potential of the 21 identified metabolites of NEE, N-terminal subunit of MGAM (NtMGAM) is used in in silico studies. The catalytic $(\beta/\alpha)_8$ domain of NtMGAM is from residues 270 to 651 with a catalytic sequence WiDMNE

which is conserved in all GH31 members. Asp443 is identified as catalytic nucleophile and Asp542 as the likely candidate for the acid/base catalysis [19].

For molecular docking studies, the crystal structure of NtMGAM (PDB ID: 2QMJ) was retrieved. All the heteroatoms were removed including glycosylated residues. Missing residues were modeled using modeler in tandem with UCSF Chimera. The 3D conformers of all the metabolites identified in the LC–MS profiling of the NEE were energy minimized using HyperChem-7. All the files were converted to PDB format. Docking was performed using the AutoDock Vina plugin of Pymol [20, 21]. By using the Lamarckian genetic algorithm (LGA) of the AutoDock Vina plugin of Pymol, the docking (ligand fitting and scoring function) was performed [22]. Rigid docking (grid-specific) operation was carried out in a box with dimensions 29.184, 29.795, and 25.404 and a grid centered around the residues of the active site. The programme was run using default settings, with a minimum population size of 100. The ligand with the best pose was selected based on binding energy. Further analysis of the interactions was studied using Ligplot + .

Results and Discussions

Identification of the Endophytic Fungus

Among the four endophytic fungi, *Nigrospora sphaerica* BRN 01 (ID: OP295074), *Nigrospora sphaerica* BRN 02 (ID: OQ377130), *Annulohypoxylon* sp. BRN 03 (ID: OQ377131), and *Colletotrichum* sp. BRN 04 (ID: OQ377132), that were identified, *Nigrospora sphaerica* BRN 01 was selected for further studies as it showed significant antioxidant as well as anti-glucosidase activity. The phylogenetic analysis of *Nigrospora sphaerica* BRN 01 was carried out. In the phylogenetic tree (Fig. 1), the optimal tree is displayed with a branch length sum of 0.09117917. The percentage of replicate trees where the associate taxa are grouped together in the bootstrap test is also provided next to the branches (1000 replicates).

Antioxidant Assay

There has recently been a renewed interest worldwide in finding natural antioxidants with minimal or no negative effects for use in preventative medicine. Reactive oxygen species (ROS), a crucial factor in the development of many diseases such as atherosclerosis, coronary heart disease, and diabetes, are combated by antioxidant chemicals, which have a significant positive impact on health [23]. One of the main explanations put forth to explain development of diabetes due to hyperglycemia is impaired equilibrium between reactive oxygen species capacity and antioxidant defense capability. Therefore, utilizing antioxidant compounds can be useful for removing different reactive oxygen species and preventing diabetes mellitus. Specific goal is to get medications that have antioxidant activity as well as antidiabetic activity [24].

Ethyl acetate extracts of endophytic fungi isolated from *B. purpurea* were screened for their antioxidant potential. Antioxidant activity was evaluated using two methods: DPPH and FRAP assays. At 200 µg/ml, NEE exhibited maximum DPPH radical activity at 92%, whereas ethyl acetate extracts of other endophytic fungi *Colletotrichum* sp. (CEE), *Annulohypoxylon* sp. (AEE), and *Nigrospora sphaerica* BRN 02 (NEE2) showed 72%, 18%, and 8%, respectively (Fig. 2). DPPH radical scavenging activity of the NEE showed 90%

Fig. 1 Phylogenetic tree

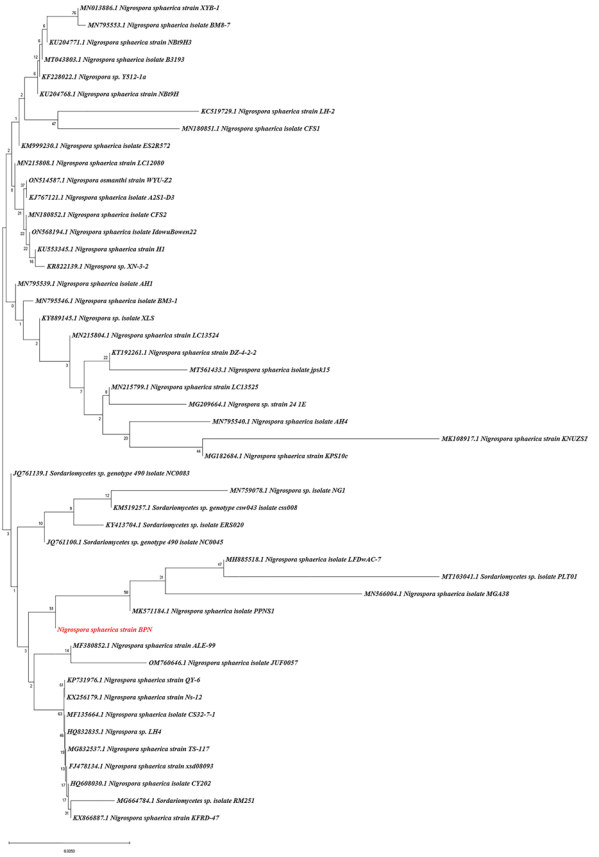

inhibition at a concentration as low as 30 µg/ml. So, NEE was selected for calculating IC50. The IC50 value of NEE was significant at 9.72 ± 0.91 µg/ml and comparable with that of positive control ascorbic acid (7.15 ± 0.15 µg/ml) as given in the supplementary data S1. The IC50 value of NEE obtained was comparable with corresponding results obtained using various plant extracts as well as metabolites isolated [25–28]. Antioxidant activity of NEE by FRAP assay was significant at 1595 µmol AAE g^{-1} DW of NEE (ascorbic acid equivalence per gram dry weight of NEE).

α-Glucosidase Inhibition Assay

Enzyme α-glucosidase located in the small intestine breaks down carbohydrates into glucose. Targeting this enzyme is an effective way to control postprandial hyperglycemia and thereby reduce the risk of heart diseases [29].

Ethyl acetate extracts of endophytic fungi isolated from *B. purpurea* were screened for their α-glucosidase inhibition potential. At 50 µg/ml, NEE showed the best inhibition activity at 93% along with best antioxidant activity. NEE2, AEE, and CEE exhibited 75.40%, 10.55%, and 9.96%, respectively (Fig. 3). So, NEE was selected for IC50 calculation. The IC50 value of NEE was 0.020 ± 0.001 mg/ml, significantly greater than the standard drug acarbose (0.494 ± 0.009 mg/ml) as given in the supplementary data S1.

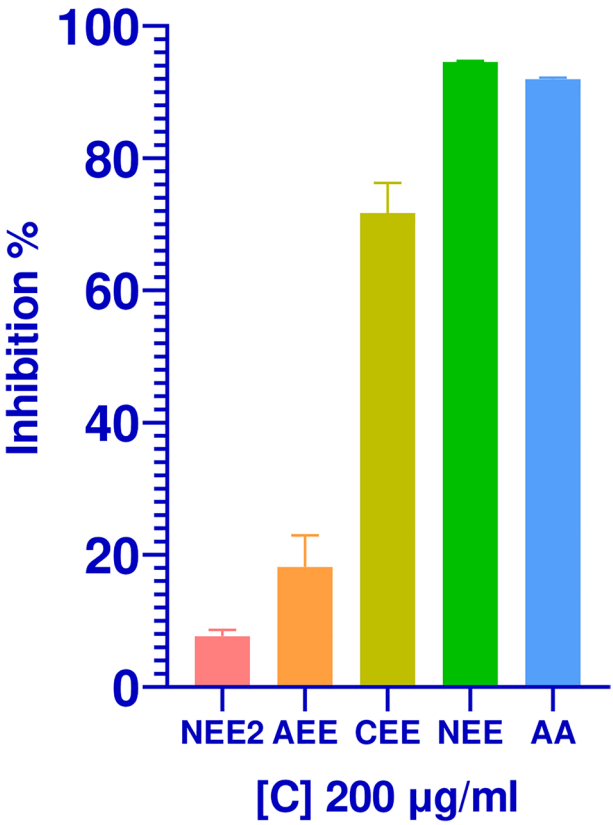

Fig. 2 DPPH radical scavenging activity of NEE, NEE2, AEE, CEE, and positive control AA at 200 µg/ml. Created by GraphPad Prism V 8.0.1

NEE showed excellent antioxidant as well as α-glucosidase inhibition which could prove to be a good source of bioactive metabolites with dual functions. Metabolite profiling of NEE was carried out to get insights on the bioactive molecules which could be acting as antioxidant agents as well as inhibitors of α-glucosidase.

Nigrospora sphaerica isolated from *Helianthus annuus* was reported to inhibit α-glucosidase with an IC50 value of 17.25 µg/ml [30]. However, antioxidant studies and detailed metabolite profiling were not carried out. This is being attempted in the current study.

Cytotoxicity Assay

Cytotoxicity of NEE was studied in the concentration range of 50–1000 µg/ml. IC 50 of NEE was 225.35 µg/ml (Fig. 4). Since IC50 value of NEE is above 100 µg/ml, it is not cytotoxic [31]. When a compound's IC50 is more than 90 µg/ml, it is reported to be safe [31, 32].

Metabolite Profiling Using UHPLC–QTOF-MS

Profiling of the NEE was carried out using UHPLC-ESI-QTOF-MS/MS. Total ion chromatogram (TIC) and base peak chromatogram (BPC) were obtained from the LC–MS scan. MS scan was performed using both positive and negative ionization

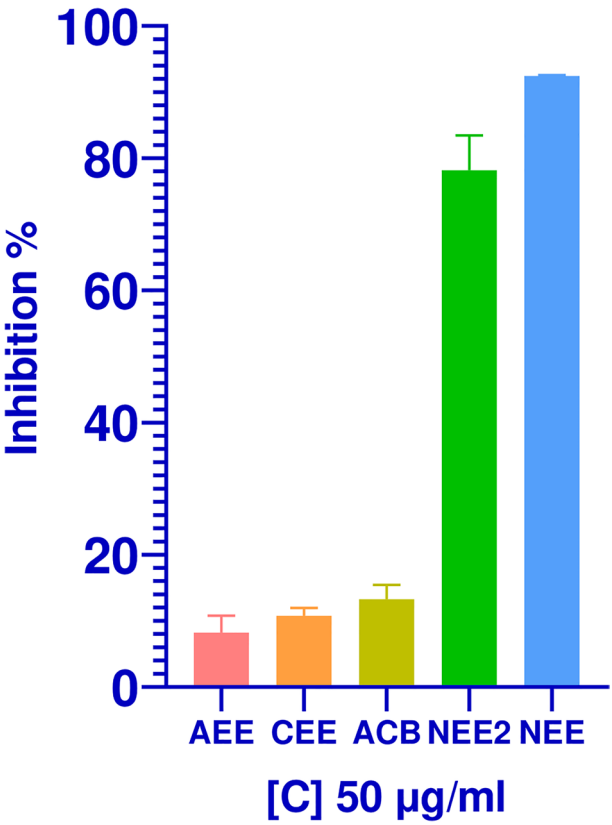

Fig. 3 α-Glucosidase inhibition potential of NEE, NEE2, AEE, CEE, and positive control ACB at 50 µg/ml. Created by GraphPad Prism V 8.0.1

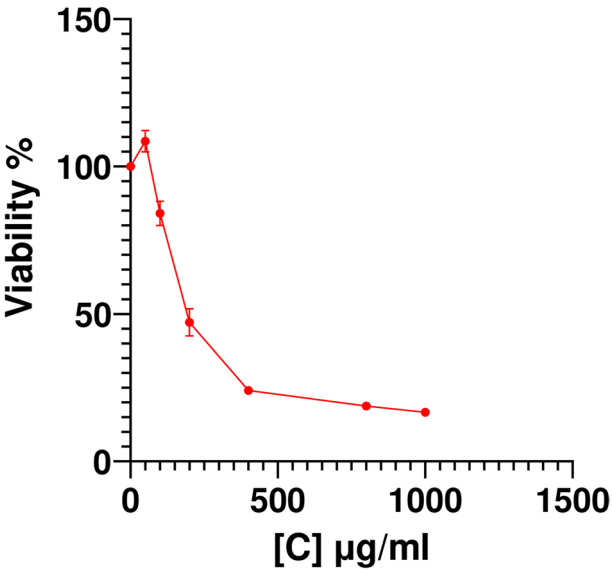

Fig. 4 Effect of NEE on cell viability of RAW 264.7 macrophage cell lines

modes. Metabolites present in the crude extracts were identified from the MS/MS data by comparing them with the PCDL library containing 850 metabolites. Ten metabolites were identified in ESI positive mode and 11 metabolites from negative ionization mode as shown in Tables 1 and 2. These metabolites were detected with a score above 75% of the isotopic pattern. The error in mass of the identified molecules was below 5 ppm. In Fig. 5, TIC scans of both types are displayed. Tables 1 and 2 contain a list of the identified metabolites, along with information on their formulae, experimental m/z, retention time (RT), and MS/MS fragments. MS/MS fragments obtained were analyzed using MetFrag in silico fragmenter [33]. Spectrum of each of the compounds along with the fragmentation pattern is provided in the supplementary data S2.

In the positive ionization mode, based on the area under peak, the most abundant molecules were protocatechuic acid, phenylethyl alcohol, (R)-ethyl 3,5-dihydroxy-7-(8-hydroxynonyl) benzoate, cyclo-(L-Ile-L-Pro), and 4-hydroxybenzaldehyde with each having a score above 90%. In the negative ionization mode, abundant molecules based on the area under peak were protocatechuic acid and mellein. Most of the secondary metabolites identified belong to polyphenols, polyketides, lactones, isocoumarin, and diketopiperazines.

In the positive ionization mode, Compound **1** was identified as protocatechuic acid with a diagnostic MS2 fragment at m/z 109 and other characteristic fragments at m/z 137 and 81 [34]. Protocatechuic acid is a natural phenolic molecule with good antioxidant activity [35]. It is also reported to have significant α-glucosidase inhibition potential (IC50 = 1.76 μM) [36]. In the negative ionization mode, Compound **11** was identified as protocatechuic acid with parent ion at m/z 153 and other characteristic fragments at m/z 108, 109, 123, and 136 [37]. (R)-ethyl 3,5-dihydroxy-7-(8-hydroxynonyl) benzoate (Compound **10**) is a derivative of protocatechuic acid which exhibited potent inhibitory activity against α-glucosidase activity in vitro with an IC50 of 22.3 μM [38]. Other derivatives include (E)-9-ethenolasiodiplodin (Compound **20**) and lasicicol (Compound **21**) with IC50 of 10.1 μM and 35.9 μM, respectively. In MetFrag analysis, Compound **1** matched with 9 fragments generated in silico. Compounds **11**, **10**, **20**, and **21** matched with 12 fragments, 7 fragments, 17 fragments, and 11 fragments generated in silico for the respective molecules.

Nigrospora sp. is known to produce several diketopiperazines (DKPs) [39]. DKPs identified in positive ionization mode included cyclo(L-Pro-L-Val), cyclo-(L-Ile-L-Pro), and cyclo[L-(4-hydroxyprolinyl)-L-Leu]. Since MS2 fragments with m/z 72.0803, 98.0593, 124.1111, 154.0722, and 169.1306 reported for cyclo(Pro-Val) were observed in experimental MS2 fragments of Compound **3**, the latter was identified as cyclo(Pro-Val). Compound **5** was identified as cyclo-(L-Ile-L-Pro) since fragments with m/z 70.0649, 86.0959, and 98.0596 matched with findings already published [40]. Twelve fragments generated by MetFrag for cyclo[L-(4-hydroxyprolinyl)-L-Leu] matched with MS2 fragments of Compound **6** and, therefore, identified as cyclo[L-(4-hydroxyprolinyl)-L-Leu].

One of the characteristic ions of 3-methoxynobiletin reported at m/z 373.0909 [41] was observed in the MS2 fragments of Compound **7**. Seventeen fragments of Compound **7** were matching with in silico fragments obtained through MetFrag. Hence, Compound **7** was identified as 3-methoxynobiletin. Two possible fragments which could be obtained from hydroxybenzaldehyde at m/z 95.0486 and 77.0381 were observed in MS2 fragments of Compound **9** and, therefore, identified as hydroxybenzaldehyde. MetFrag generated 24, 6, and 21 fragments for 12-methoxycitromycin, Phenylethyl alcohol and Pestalafuranone G which were matching with fragments generated for the compounds **4**, **6**, and **8** respectively. Pestalafuranones G was previously reported to be produced by *Nigrospora* sp. [42].

Table 1 Identified compounds along with retention time, molecular formula, observed mass, and MS/MS fragment masses

No	Retention time (min)	Molecular formula	Compounds identified	Observed mass (m/z)	MS/MS fragment masses
1	2.982	$C_7H_6O_4$	Protocatechuic acid	137.0228	81.0328, 109.0281, 137.0223
2	8.098	$C_{10}H_{16}N_2O_2$	Cyclo(L-Pro-L-Val)	197.1275	70.0643, 72.0802, 154.0737, 169.1383
3	8.719	$C_{11}H_{18}N_2O_3$	Cyclo[L-(4-hydroxyprolinyl)-L-Leu]	227.1379	68.0485, 86.0589, 114.0537, 199.1443
4	10.297	$C_{14}H_{12}O_5$	12-Methoxycitromycin	261.0744	83.0485, 139.0381, 159.0424, 215.0694
5	10.661	$C_{11}H_{18}N_2O_2$	Cyclo-(L-Ile-L-Pro)	211.1433	70.0649, 86.0959, 98.0596, 183.1486
6	13.234	$C8H_{10}O$	Phenylethyl alcohol	105.0695	77.0383, 91.0530, 105.0694
7	16.614	$C_{22}H_{24}O_9$	3-Methoxynobiletin	415.1379	53.0368, 137.0216, 155.0330, 373.0933
8	22.734	$C_{11}H_{16}O_3$	Pestalafuranones G	197.1164	67.0535, 81.0691, 123.1157, 133.1006
9	25.758	$C_7H_6O_2$	4-Hydroxybenzaldehyde	123.0436	55.0166, 67.0542, 77.0381, 95.0486
10	40.395	$C_{18}H_{28}O_5$	(R)-ethyl 3,5-dihydroxy-7-(8-hydroxynonyl) benzoate	307.1891	71.0844, 121.0263, 149.0220, 309.1709

Table 2 Identified compounds along with retention time, molecular formula, observed mass, and MS/MS fragments

No	Retention time (min)	Molecular formula	Compounds identified	Observed mass (m/z)	MS/MS fragment masses (m/z)
11	8.669	$C_7H_6O_4$	Protocatechuic acid	153.0194	107.0126, 109.0293, 123.0082, 137.0246
12	10.431	$C_{16}H_{20}O_9$	Feruloyl glucose	401.1084	148.0536, 192.0428, 275.0554, 282.0767
13	11.047	$C_{10}H_{12}O_2$	Eugenol	191.0714	107.0509, 122.0665, 135.0431, 148.0517
14	11.487	$C_{14}H_{16}O_4$	1-(5-Oxotetrahydrofuran-2-yl) ethyl 2-phenylacetate	275.0988	108.0215, 121.0288,135.0449, 152.0474
15	11.947	$C_{14}H_{14}O_4$	5′-Methoxy-6-methyl-biphenyl-3,4,3′-triol	245.0823	108.0120, 122.0382, 135.0448, 229.0526
16	14.863	$C_{20}H_{18}O_6$	Pulvinone P	399.1087	111.0446, 135.0446, 243.0673
17	18.043	$C_{10}H_{10}O_4$	Mellein	177.0557	107.0487, 120.0218, 133.0656, 148.0160
18	18.761	$C_{10}H_8O_4$	5,8-Dihydroxy-4-methyl-coumarin	191.0346	138.0323, 149.0242, 176.0114
19	20.221	$C_{11}H_{16}O_4$	Pestalafuranones I	211.0981	104.9974, 111.0827, 167.1082
20	26.158	$C_{17}H_{22}O_4$	(E)-9-etheno-lasiodiplodin	335.1504	109.0284, 139.0409, 169.1242, 195.1049
21	30.845	$C_{18}H_{24}O_5$	Lasicicol	319.1555	111.0801, 138.0328, 169.1233. 195.1027, 213.117

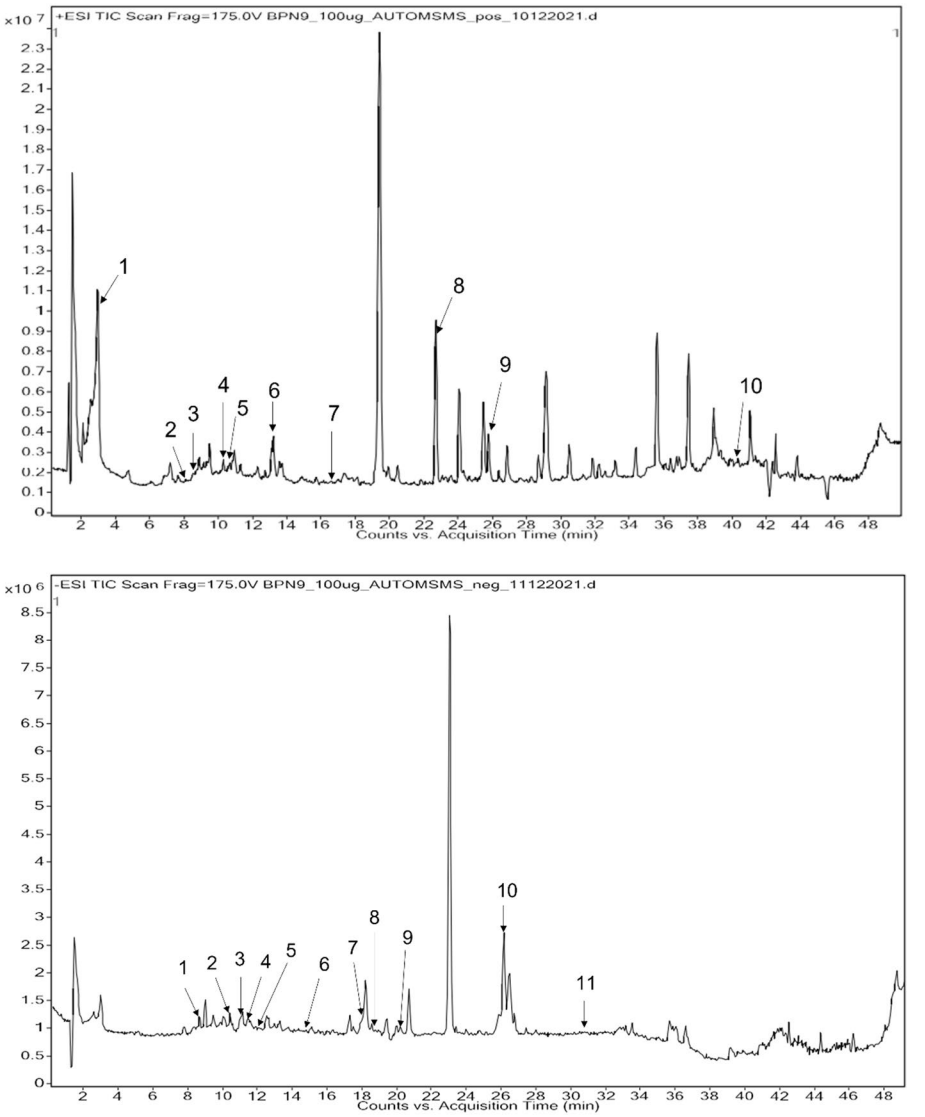

Fig. 5 Extracellular secondary metabolites detected in NEE by UHPLC–QTOF-MS (positive and ionization mode)

Three of the MS2 fragments generated by Compound **13** matched with fragments at m/z 105, 109, and 133 reported from eugenol [43]. Furthermore, 16 MetFrag-generated fragments of eugenol were matching with fragments of Compound **13**. This compound was identified as eugenol. Based on MetFrag analysis, Compound **12** with a match of 19 fragments, Compound **14** with 26 fragments, Compound **15** with 11 fragments, Compound **16** with 31 fragments, Compound **17** with 12 fragments, Compound **18** with 10 fragments, and Compound **19** with 7 fragments were identified as feruloyl glucose, eugenol, 1-(5-oxotetrahydrofuran-2-yl)ethyl 2-phenylacetate,

5′-methoxy-6-methyl-biphenyl-3,4,3′-triol, pulvinone P, mellein 5,8-dihydroxy-4-methyl-coumarin, and pestalafuranones I, respectively. Pestalafuranones I were previously reported to be produced by *Nigrospora* sp. [42].

Protocatechuic acid and its derivatives known for their antioxidant and α-glucosidase inhibition potential were the most abundant molecules in the NEE. They were probably the major contributors for significant antioxidant and antidiabetic activities observed.

Molecular Docking

Molecular docking studies of all the 21 metabolites identified in the LC–MS studies were carried out. Six metabolites had higher binding energy than that of the standard drug acarbose. According to Zhang et al. [44], stabilization of the enzyme and ligand molecule complex in catalytic processes depends heavily on hydrogen bond interactions. In the Ligplot + analysis, acarbose forms hydrogen bonds with His600, Asp327, Asp443, Arg334, and Trp406. Interaction of feruloyl glucose with the active site residues is analyzed using Pymol and Protein–Ligand Interaction Profiler and shown in Fig. 6. Based on Ligplot + analysis, feruloyl glucose, a dietary polyphenol, showed hydrogen bonding interactions with residues Asp203, Asp327, and Thr205 and with the key residue Asp542 which is conserved through GH31 family and is involved in acid/

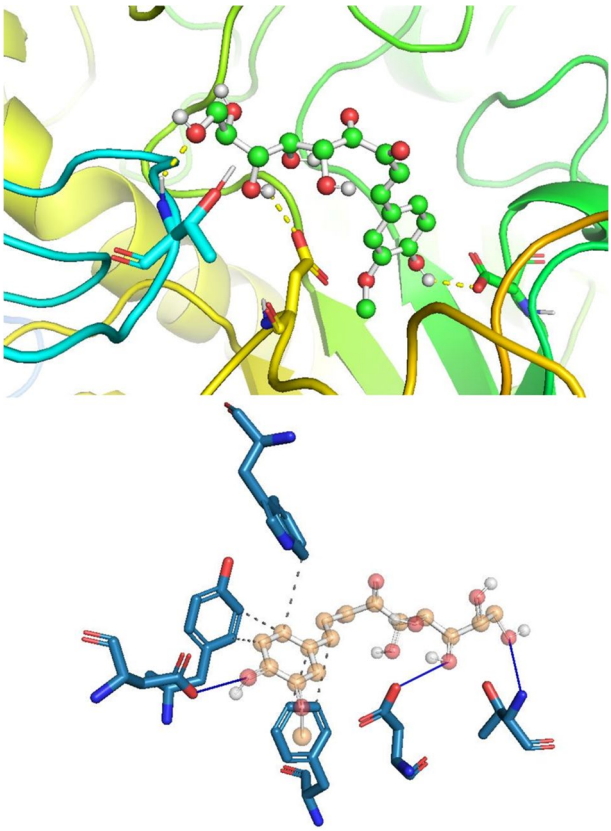

Fig. 6 Hydrogen bonding and hydrophobic interactions of feruloyl glucose with the active site of α-glucosidase. Created by Pymol and Protein–Ligand Interaction Profiler

Table 3 Binding energies of the ligands with higher binding affinity than standard drug, acarbose

Sl. no	Compound	Binding energy (kcal/mol)	Residues involved in hydrogen bonding
1	Pulvinone P	−7.2	His600, Asp327, Arg526
2	Feruloyl glucose	−7	Asp327, Asp542, Asp203, Thr205
3	Lasicicol	−6.9	-
4	De-O-methyllasiodiplodin	−6.9	Arg526
5	Mellein	−6.9	Asp443, Arg526
6	(R)-ethyl 3,5-dihydroxy-7-(8-hydroxynonyl) benzoate	−6.6	Asp443, Asp542, Tyr605, Gln603
7	Acarbose	−6.6	His600, Asp327, Asp443, Arg334, Trp406
8	Protocatechuic acid	−6.4	Asp327, Arg526

base catalysis [19]. Feruloyl glucose also forms hydrophobic interactions with active site residues Tyr299, Trp406, and Phe575. Although pulvinone P had the highest binding energy, it had a smaller number of hydrogen bond interaction with the target than feruloyl glucose. So feruloyl glucose could be a potential AGI and was selected for further studies. Binding energies of the 6 ligands with higher binding affinity compared to that of the standard drug, acarbose, along with their hydrogen bond interactions are given in Table 3. Ligplot + analysis of all these ligands with the catalytic site of α-glucosidase is provided in the supplementary data S3. Purification and confirming the potential of these metabolites as AGI through in vivo studies would be the next step.

Supplementary Information The online version contains supplementary material available at https://doi.org/10.1007/s12010-023-04452-7.

Acknowledgements The authors are ever grateful to the Founder Chancellor, Sri Sathya Sai Institute of Higher Learning (SSSIHL), Bhagawan Sri Sathya Sai Baba, for constant guidance and support. The authors are thankful to SSSIHL and UGC-SAP for providing financial support to carry out this work. The authors are grateful to Central Research Instrumentation Facility (CRIF), SSSIHL, for providing all necessary facilities. The authors wish to thank V. N. Ravi Kishore Vutukuri for the help provided in optimizing mass spectrometry protocols.

Author Contribution Sai Anand Kannakazhi Kantari—development of methodologies and conducting investigations; data analysis and data presentation and writing the original draft.
Ranendra Pratap Biswal—development of methodology for LC–MS analysis.
Piyush Kumar—participated in conducting investigations.
Malleswara Dharanikota—providing some resources.
Ashok Agraharam—conception or design of the work, writing (review and editing), supervision.

Data Availability Data will be made available on request.

Declarations

Ethical Approval Not applicable.

Consent to Participate Not applicable.

Consent for Publication Not applicable.

Competing Interests The authors declare no competing interests.

References

1. IDF Diabetes Atlas | Tenth Edition. (n.d.). Retrieved from https://diabetesatlas.org/
2. Hossain, U., Das, A. K., Ghosh, S., & Sil, P. C. (2020). An overview on the role of bioactive α-glucosidase inhibitors in ameliorating diabetic complications. *Food and Chemical Toxicology, 145*, 111738. https://doi.org/10.1016/J.FCT.2020.111738
3. Riyaphan, J., Pham, D. C., Leong, M. K., & Weng, C. F. (2021). In silico approaches to identify polyphenol compounds as α-glucosidase and α-amylase inhibitors against type-II diabetes. *Biomolecules, 11*(12), 1877. https://doi.org/10.3390/BIOM11121877
4. Akmal, M., & Wadhwa, R. (2022). Alpha glucosidase inhibitors. *NCBI Bookshelf*. Retrieved from https://www.ncbi.nlm.nih.gov/books/NBK557848/
5. Smith, D. L., Orlandella, R. M., Allison, D. B., & Norian, L. A. (2021). Diabetes medications as potential calorie restriction mimetics—A focus on the alpha-glucosidase inhibitor acarbose. *GeroScience, 43*(3), 1123–1133. https://doi.org/10.1007/S11357-020-00278-X/FIGURES/1
6. Uuh Narvaez, J. J., & Segura Campos, M. R. (2022). Combination therapy of bioactive compounds with acarbose: A proposal to control hyperglycemia in type 2 diabetes. *Journal of Food Biochemistry*, e14268. https://doi.org/10.1111/JFBC.14268
7. Dirir, A. M., Daou, M., Yousef, A. F., & Yousef, L. F. (2021). A review of alpha-glucosidase inhibitors from plants as potential candidates for the treatment of type-2 diabetes. *Phytochemistry Reviews, 21*(4), 1049–1079. https://doi.org/10.1007/S11101-021-09773-1
8. Wen, J., Okyere, S. K., Wang, S., Wang, J., Xie, L., Ran, Y., & Hu, Y. (2022). Endophytic fungi: An effective alternative source of plant-derived bioactive compounds for pharmacological studies. *Journal of Fungi, 8*(2), 205. https://doi.org/10.3390/JOF8020205
9. Benjamim, J., da Costa, K., Santos, A., & Santos, A. (2021). Chemical, botanical and pharmacological aspects of the Leguminosae. *Pharmacognosy Reviews, 14*(28), 106–120. https://doi.org/10.5530/phrev.2020.14.15
10. Xu, T., Song, Z., Hou, Y., Liu, S., Li, X., Yang, Q., & Wu, S. (2022). Secondary metabolites of the genus Nigrospora from terrestrial and marine habitats: Chemical diversity and biological activity. *Fitoterapia, 161*, 105254. https://doi.org/10.1016/J.FITOTE.2022.105254
11. Suryanarayanan, T. S., Kumaresan, V., & Johnson, J. A. (1998). Foliar fungal endophytes from two species of the mangrove Rhizophora. *Canadian Journal of Microbiologyicrobiology, 44*(10), 1003–1006. https://doi.org/10.1139/W98-087
12. Sharma, D., Pramanik, A., & Agrawal, P. K. (2016). Evaluation of bioactive secondary metabolites from endophytic fungus Pestalotiopsis neglecta BAB-5510 isolated from leaves of Cupressus torulosa D.Don. *3 Biotech*, *6*(2). https://doi.org/10.1007/S13205-016-0518-3
13. Kumar, S., Stecher, G., Li, M., Knyaz, C., & Tamura, K. (2018). MEGA X: Molecular evolutionary genetics analysis across computing platforms. *Molecular biology and evolution, 35*(6), 1547–1549. https://doi.org/10.1093/MOLBEV/MSY096
14. Tamura, K., Nei, M., & Kumar, S. (2004). Prospects for inferring very large phylogenies by using the neighbor-joining method. *Proceedings of the National Academy of Sciences of the United States of America, 101*(30), 11030–11035. https://doi.org/10.1073/PNAS.0404206101/ASSET/D0B973E3-6167-4566-B866-7A0FB0A0057B/ASSETS/GRAPHIC/ZPQ0300455080006.JPEG
15. Bulut, O., Akın, D., Sönmez, Ç., Öktem, A., Yücel, M., & Öktem, H. A. (2019). Phenolic compounds, carotenoids, and antioxidant capacities of a thermo-tolerant Scenedesmus sp. (Chlorophyta) extracted with different solvents. *Journal of Applied Phycology, 31*(3), 1675–1683. https://doi.org/10.1007/S10811-018-1726-5/TABLES/4
16. Khor, B.-K., Jeng-YeouChear, N., Azizi, J., Khaw, K.-Y., Khor, B.-K., Chear, N., & Chemical, K.-Y. (2021). Chemical composition, antioxidant and cytoprotective potentials of Carica papaya leaf extracts: A comparison of supercritical fluid and conventional extraction methods. *Molecules, 26*(5), 1489. https://doi.org/10.3390/MOLECULES26051489
17. Bhatia, A., Singh, B., Arora, R., & Arora, S. (2019). In vitro evaluation of the α-glucosidase inhibitory potential of methanolic extracts of traditionally used antidiabetic plants. *BMC Complementary and Alternative Medicine*, *19*(1). https://doi.org/10.1186/s12906-019-2482-z
18 Biswal, R. P., Dandamudi, R. B., Patnana, D. P., Pandey, M., & Vutukuri, V. N. R. K. (2022). Metabolic fingerprinting of Ganoderma spp using UHPLC-ESI-QTOF-MS and its chemometric analysis. *Phytochemistry, 199*, 113169. https://doi.org/10.1016/J.PHYTOCHEM.2022.113169
19. Sim, L., Quezada-Calvillo, R., Sterchi, E. E., Nichols, B. L., & Rose, D. R. (2008). Human intestinal maltase–glucoamylase: Crystal structure of the N-terminal catalytic subunit and basis of inhibition and substrate specificity. *Journal of Molecular Biology, 375*(3), 782–792. https://doi.org/10.1016/J.JMB.2007.10.069

20. Seeliger, D., & De Groot, B. L. (2010). Conformational transitions upon ligand binding: Holo-structure prediction from apo conformations. *PLoS Computational Biology*, *6*(1). https://doi.org/10.1371/JOURNAL.PCBI.1000634
21. Trott, O., & Olson, A. J. (2010). AutoDock Vina: Improving the speed and accuracy of docking with a new scoring function, efficient optimization, and multithreading. *Journal of Computational Chemistry, 31*(2), 455–461. https://doi.org/10.1002/JCC.21334
22. Ghanta, P., Sinha, S., Doble, M., & Ramaiah, B. (2020). Potential of pyrroquinazoline alkaloids from Adhatoda vasica Nees. as inhibitors of 5-LOX – a computational and an in-vitro study. https://doi.org/10.1080/07391102.2020.1848635, *40*(6), 2785–2796. https://doi.org/10.1080/07391102.2020.1848635
23. Hyun, T. K., Kim, H. C., & Kim, J. S. (2014). Antioxidant and antidiabetic activity of Thymus quinquecostatus Celak. *Industrial Crops & Products*, *Complete*(52), 611–616. https://doi.org/10.1016/J.INDCROP.2013.11.039
24. Giacco, F., & Brownlee, M. (2010). Oxidative stress and diabetic complications. *Circulation research, 107*(9), 1058. https://doi.org/10.1161/CIRCRESAHA.110.223545
25 Erenler, R., Telci, I., Ulutas, M., Demirtas, I., Gul, F., Elmastas, M., & Kayir, O. (2015). Chemical constituents, quantitative analysis and antioxidant activities of Echinacea purpurea (L.) Moench and Echinacea pallida (Nutt.) Nutt. *Journal of Food Biochemistry, 39*(5), 622–630. https://doi.org/10.1111/JFBC.12168
26. Erenler, R., Sen, O., Aksit, H., Demirtas, I., Yaglioglu, A. S., Elmastas, M., & Telci, I. (2016). Isolation and identification of chemical constituents from Origanum majorana and investigation of antiproliferative and antioxidant activities. *Journal of the Science of Food and Agriculture, 96*(3), 822–836. https://doi.org/10.1002/JSFA.7155
27. Visavadiya, N. P., Soni, B., & Dalwadi, N. (2009). Evaluation of antioxidant and anti-atherogenic properties of Glycyrrhiza glabra root using in vitro models. *International Journal of Food Sciences and Nutrition, 60*(SUPPL. 2), 135–149. https://doi.org/10.1080/09637480902877998
28. Rigane, G., Ghazghazi, H., Aouadhi, C., Ben Salem, R., & Nasr, Z. (2017). Phenolic content, antioxidant capacity and antimicrobial activity of leaf extracts from Pistacia atlantica. *Natural Product Research, 31*(6), 696–699. https://doi.org/10.1080/14786419.2016.1212035
29. Nadeem, M., Mumtaz, M. W., Danish, M., Rashid, U., Mukhtar, H., & Irfan, A. (2020). Antidiabetic functionality of Vitex negundo L. leaves based on UHPLC-QTOF-MS/MS based bioactives profiling and molecular docking insights. *Industrial Crops and Products, 152*, 112445. https://doi.org/10.1016/J.INDCROP.2020.112445
30. Supaphon, P., & Preedanon, S. (2019). Evaluation of in vitro alpha-glucosidase inhibitory, antimicrobial, and cytotoxic activities of secondary metabolites from the endophytic fungus, Nigrospora sphaerica, isolated from Helianthus annuus. *Annals of Microbiology, 69*(13), 1397–1406. https://doi.org/10.1007/S13213-019-01523-1/TABLES/3
31. Sharaf, M. H., Abdelaziz, A. M., Kalaba, M. H., Radwan, A. A., & Hashem, A. H. (2022). Antimicrobial, antioxidant, cytotoxic activities and phytochemical analysis of fungal endophytes isolated from Ocimum Basilicum. *Applied Biochemistry and Biotechnology, 194*(3), 1271–1289. https://doi.org/10.1007/S12010-021-03702-W/FIGURES/6
32. Robert, J. -, & Yardley, V. (2009). *Drugs for neglected diseases initiative (DNDi)*. Swiss Tropical Institute (STI), Tanja Wenzler, Swiss Tropical Institute (STI): Reto Brun.
33. Ruttkies, C., Schymanski, E. L., Wolf, S., Hollender, J., & Neumann, S. (2016). MetFrag relaunched: Incorporating strategies beyond in silico fragmentation. *Journal of Cheminformatics*, *8*(1). https://doi.org/10.1186/S13321-016-0115-9
34. Nadeem, M., Mumtaz, M. W., Danish, M., Rashid, U., Mukhtar, H., & Irfan, A. (2020). Antidiabetic functionality of Vitex negundo L. leaves based on UHPLC-QTOF-MS/MS based bioactives profiling and molecular docking insights. *Industrial Crops and Products, 152*(April), 112445. https://doi.org/10.1016/j.indcrop.2020.112445
35. Tanaka, T., Tanaka, T., & Tanaka, M. (2011). Potential cancer chemopreventive activity of protocatechuic acid. *Journal of Experimental and Clinical Medicine, 3*(1), 27–33. https://doi.org/10.1016/J.JECM.2010.12.005
36. Adefegha, S. A., Oboh, G., Ejakpovi, I. I., & Oyeleye, S. I. (2015). Antioxidant and antidiabetic effects of gallic and protocatechuic acids: A structure–function perspective. *Comparative Clinical Pathology, 24*(6), 1579–1585. https://doi.org/10.1007/S00580-015-2119-7/FIGURES/7
37. Kramberger, K., Barlič-Maganja, D., Bandelj, D., BarucaArbeiter, A., Peeters, K., MiklavčičVišnjevec, A., & Pražnikar, Z. J. (2020). HPLC-DAD-ESI-QTOF-MS determination of bioactive compounds and antioxidant activity comparison of the hydroalcoholic and water extracts from two Helichrysum italicum species. *Metabolites, 10*(10), 1–25. https://doi.org/10.3390/METABO10100403

38. Chen, S., Liu, Z., Li, H., Xia, G., Lu, Y., He, L., & She, Z. (2015). β-Resorcylic acid derivatives with α-glucosidase inhibitory activity from Lasiodiplodia sp. ZJ-HQ1, an endophytic fungus in the medicinal plant Acanthus ilicifolius. *Phytochemistry Letters, 13*, 141–146. https://doi.org/10.1016/j.phytol.2015.05.019
39. Huang, D. Y., Nong, X. H., Zhang, Y. Q., Xu, W., Sun, L. Y., Zhang, T., … Han, C. R. (2021). Two new 2,5-diketopiperazine derivatives from mangrove-derived endophytic fungus Nigrospora camelliae-sinensis S30. https://doi.org/10.1080/14786419.2021.1878168. https://doi.org/10.1080/14786419.2021.1878168
40. Zhang, F., Li, B., Wen, Y., Liu, Y., Liu, R., Liu, J., & Jiang, Y. (2022). An integrated strategy for the comprehensive profiling of the chemical constituents of Aspongopus chinensis using UPLC-QTOF-MS combined with molecular networking. *Pharmaceutical Biology, 60*(1), 1349. https://doi.org/10.1080/13880209.2022.2096078
41. Lan, H. C., Li, S. Z., Li, K., & Liu, E. H. (2021). In vitro human intestinal microbiota biotransformation of nobiletin using liquid chromatography–mass spectrometry analysis and background subtraction strategy. *Journal of Separation Science, 44*(10), 2046–2053. https://doi.org/10.1002/JSSC.202001150
42. Zhang, H., Deng, Z., Guo, Z., Tu, X., Wang, J., & Zou, K. (2014). Pestalafuranones F-J, Five new furanone analogues from the endophytic fungus Nigrospora sp. BM-2. *Molecules, 19*(1), 819–825. https://doi.org/10.3390/MOLECULES19010819
43. Shen, Y., Liu, X., Yang, Y., Li, J., Ma, N., & Li, B. (2015). In vivo and in vitro metabolism of aspirin eugenol ester in dog by liquid chromatography tandem mass spectrometry. *Biomedical Chromatography, 29*(1), 129–137. https://doi.org/10.1002/BMC.3249
44 Zhang, X., Jia, Y., Ma, Y., Cheng, G., & Cai, S. (2018). Phenolic Composition, antioxidant properties, and inhibition toward digestive enzymes with molecular docking analysis of different fractions from Prinsepia utilis Royle fruits. *Molecules, 23*(12), 3373. https://doi.org/10.3390/MOLECULES23123373